 https://doi.org/10.3311/PPci.23825

Periodica Polytechnica Civil Engineering, 68(4), pp. 1052–1063, 2024

On the Buckling Response of Functionally Graded Carbon Nanotube-reinforced Composite Imperfect Beams

Sabrina Boutaleb[1], Ammar Boulal[2], Mohamed Zidour[2,3], Mohammed A. Al-Osta[4,5], Abdelouahed Tounsi[1,4,5,6*], Abdeldjebbar Tounsi[1,7], Mohamed Abdelaziz Salem[8], Khaled Mohamed Khedher[9]

[1] Material and Hydrology Laboratory, Civil Engineering Department, Faculty of Technology, University of Sidi Bel Abbes, 22000 Sidi Bel Abbes, P. O. B. 89, Algeria
[2] Laboratory of Geomatics and Sustainable Development, University of Tiaret, 14000 Tiaret, P. O. B. 78, Algeria
[3] Civil Engineering Department, University of Tiaret, 14000 Tiaret, P. O. B. 78, Algeria
[4] Department of Civil and Environmental Engineering, King Fahd University of Petroleum and Minerals, Academic Belt Road, 31261 Dhahran, Saudi Arabia
[5] Interdisciplinary Research Center for Construction and Building Materials, King Fahd University of Petroleum and Minerals, Academic Belt Road, 31261 Dhahran, Saudi Arabia
[6] Department of Civil and Environmental Engineering, Lebanese American University, 309 Bassil Building, 13-5053 Byblos, Lebanon
[7] Industrial Engineering and Sustainable Development Laboratory, Mechanical Engineering Department, Faculty of Science and Technology, University of Rélizane, 48000 Relizane, Algeria
[8] Department of Mechanical Engineering, College of Engineering, King Khalid University, 61421 Abha, P. O. B. 394, Saudi Arabia
[9] Department of Civil Engineering, College of Engineering, King Khalid University, 61421 Abha, P. O. B. 394, Saudi Arabia
* Corresponding author, e-mail: tou_abdel@yahoo.com

Received: 09 November 2023, Accepted: 17 March 2024, Published online: 07 June 2024

Abstract

The current inquiry aims to scrutinize the porosity's effect on the buckling response of carbon nanotube reinforced composite (CNTRC) imperfect beams. The developed theories account for higher-order variation of transverse shear strain through the depth of the beam and satisfy the stress-free boundary conditions on the top and bottom surfaces of the beam. Single-walled carbon nanotubes (SWCNTs) are distributed and aligned in a polymeric matrix with various reinforcement patterns to create CNTRC porous beams. The material properties of the functionally graded beam determined using the mixture rule are assumed to vary according to the power law distribution of the volume fraction of the constituents. The mathematical models presented in this study are validated through numerical comparison with existing results. The new buckling results of carbon nanotube-reinforced porous beams are analyzed considering the influence of several parameters, including volume fraction, aspect ratios, degree of porosity, and types of reinforcement. The results stipulate that the above parameters play a significant role in the critical buckling load variation. It is proclaimed that the critical buckling load dwindled as porosity increased and that the X-CNT reinforced beam has a high resistance against buckling compared to other reinforcement types.

Keywords

Functionally Graded Carbon Nanotube (FG-CNT), beam, buckling, porosity, volume fraction

1 Introduction

Due to their discovery in the last 30 years, carbone nanotubes (CNT) are among the most exciting and overwhelming new materials, owing to their mechanical properties, high elastic modulus, and low density. The why and wherefore make nanotubes excellent and peerless candidates for engineering requirements and have taken significant and noteworthy interest from the scientific community and moreover, from industry. The explosion of interest in CNTs can be traced back to a 1991 Nature paper by Sumio Iijima. Currently CNTs are the substantial subject of around seven papers per day. Deploying composite materials empowers different advantageous properties and combinations of diverse material classes, for instance, polymers. The development of fiber reinforcement in polymer matrix

Cite this article as: Boutaleb, S., Boulal, A., Zidour, M., Al-Osta, M. A., Tounsi, A., Tounsi, A., Salem, M. A., Khedher, K. M. "On the Buckling Response of Functionally Graded Carbon Nanotube-reinforced Composite Imperfect Beams", Periodica Polytechnica Civil Engineering, 68(4), pp. 1052–1063, 2024. https://doi.org/10.3311/PPci.23825

composites has been an active area of research for well over two decades due to their higher-ranking and superior mechanical, thermal, and electrical properties 1–3 [1–5]. Compared to classical carbon fiber-reinforced polymer composites, carbon nanotube-reinforced composites (CNTRCs) can greatly enhance strength and stiffness.

Functionally Graded Carbon Nanotube (FG-CNT) stands for functionally graded carbon nanotube-reinforced composite, which is a novel nanomaterial that has excellent mechanical and electrical properties. There are various technological methods used to create FG-CNT materials, each with its own advantages and limitations. The solution mixing method involves dispersing CNTs in a polymer solution and then mixing it with carbon nanotubes to form a composite [4]. The in situ polymerization method involves growing CNTs on the surface of carbon fibers and then polymerizing them with a matrix resin [5]. The electrospinning method involves spinning CNTs and polymers into nanofibers and then aligning them into a composite. By varying the solution composition and spinning parameters, a gradient in the CNT content and distribution can be obtained [6]. The layer-by-layer assembly method involves depositing CNTs and polymer layers alternately on a substrate and then peeling off the composite film [7]. This creates a gradual change in the CNT composition along the material's length. The results of Olek et al. [7] confirm the potential of the layering method for the manufacturing of composites with the high load of strong filler and the importance of uniform distribution and good interconnectivity between carbon nanotubes and the polymer matrix.

The aligned CNT arrays formed by polymer composites were explored by Ajayan et al. [8]. From then on, many researchers [9–11] studied the material characteristics of CNTRCs, GNPRCs, and graphene platelet-reinforced composite laminated. Shokrieh and Rafiee [12] analyzed the mechanical properties of carbon nanotube composites and isolated carbon nanotubes using a finite element. Srivastava et al. [13] expressed the thermal-mechanical behaviorstrain sensing of polystyrene composite films/flexible multi-walled carbon nanotubes. Alibeigloo [14] examined a thermoelastic analysis of the FG-CNTRC plate using the theory of elasticity. Hamidi et al. [15] investigated the vibration effects of embedded armchair single-walled carbon nanotubes at a small scale. Esen et al. [16] studied the free vibration and buckling stability of FG nanobeams while taking into consideration the impact of magnetic and thermal fields.

Functionally graded CNT beams have numerous practical applications, including aerospace structures, civil engineering, nuclear reactors, the biomedical industry, optical semiconductors, defense industry, automotive industry, and smart structures. These applications of (FG-CNTs) make them very attractive for many current and future engineering applications, more so than conventional carbon fiber reinforced composites. The FGNTs can also be used in the development of high-performance filtration systems. By tailoring the properties along their length, it is possible to create a gradient that filters out particles of different sizes. This can be useful in applications such as water treatment, where the removal of contaminants of different sizes is critical [17]. Another potential application of FGNTs is in energy storage and conversion. The spatial variation in material properties in FGNTs can be used to create electrodes for batteries or fuel cells with enhanced performance [18].

FG-CNT has an impact on mechanical and economic aspects. Mechanically, the graduated distribution of CNTs has proven its effect by increasing the rigidity of the beam compared to the unidirectional distribution. Note that this increase in stiffness due to the same amount of CNT used. This reinforces the importance of graduated distribution in the economic aspect. For example: the mechanical properties of the beam are improved by changing the distribution rather than increasing the volume fraction of CNTs. In current applications, reinforcement based carbon nanotubes (CNTs) have been widely adopted in place of conventional fiber [19, 20]. Wang et al. [21] analyzed the effect of fiber orientation on Young's modulus for unidirectional fiber reinforced composites.

For the combination on a microscopic scale, a novel generation of composite materials introduced in nanotechnology, which are called "Functionally Graded Materials (FGM)", has provided solutions to many technical problems in aerospace engineering [22, 23]. Adıyaman et al. [24] presented a study on the contact problem of a layer consisting of functionally graded material (FGM) in the presence of body force. Yaylacı et al. [22] evaluated the contact problem of a functionally graded layer resting on a rigid foundation pressed via a rigid punch by analytical and numerical (FEM and MLP) methods. The contact problem of the functionally graded layer resting on a rigid foundation pressed via a rigid punch has been studied by Yaylacı et al. [25].

The combination of MD simulations and continuum mechanics provides a comprehensive understanding of nanocomposite materials. MD simulations provide insight into the behavior of CNTs and their interactions with the matrix at the nanoscale, while continuum mechanics provides a macroscopic description of the mechanical

properties [26–28]. Other methods, like finite element and artificial neural network methods, were used to analyze the contact problem of a functionally graded layer [29, 30]. Öner et al. [31] investigated the contact between two functionally graded layers on the plane receding using computational, finite element, and artificial neural network methods. Edge and an internal crack problem and estimation of the stress intensity factor through the finite element method are used by Yaylaci [32].

Nonetheless, composite manufacturing processes are complex and can lead to the occurrence, evolution and build out of defects, for instance, porosity, which influences structure mechanical properties. A porosity defect is elucidated by the presence of small cavities, which contain gaseous matter called pores and are classified according to their size (micro, meso, and macro-pores). This shortcoming is due to inappropriate air extraction ascribed to miscellaneous constants such as the viscosity of the matrix, vacuum pressure, or humidity of the material. A recent study by Sisodia et al. [33] involved the effects of voids on the quasi-static and tension fatigue behavior of carbon-fiber composite laminates. Using analytical, finite element, and artificial neural network methods, Turan et al. [34] present the free vibration and buckling of functionally graded porous beams.

The existence of porosity in composite parts is an unavoidable fact. Consequently, limits have been fixed in obedience to the applications: in aerospace, structures work forcefully. Moreover, it's not tolerable when the porosity rate exceeds 1% [35], dissimilar to other applications where a level of 5% or more can be tolerated [36]. In the current analysis of fully isolated pores of nearly spherical or elliptical shape, the rate of porosities used doesn't exceed 4%.

For these applications, polymer behavior analysis with porosity is foremost and essential because porosity increases, which is usually accompanied by alterations in the polymer's mechanical properties. Carbon nanotubes superlatives lend a hand to an excellent build-up for polymer matrix. Wan et al. [37] supported this argument, as they conducted an analysis on the effective moduli of CNT-reinforced polymer composites, with a focus on the impact of CNT length and CNT matrix interphase on the overall stiffening of the composite material. On the other hand, the functionally graded distributions of carbon nanotube (FG-CNT) along the thickness direction with and without porosity have been widely investigated in recent years [38, 39]. Yaylacı et al. [40] Studied the vibration and buckling analyses of FGM beam with edge crack: Finite element and multilayer perception methods.

The buckling behavior of beams is significantly affected by the alignment and distribution of single-walled carbon nanotubes (SWCNTs) in a polymeric matrix with varying reinforcement patterns. The material properties of the CNTRC porous beams are gauged using the mixture rule. The righteous agreement and concord between the current query results and those available within easy reach in the literature endorse the introduced approach. The critical buckling loads for porous beams are presented and bestowed with changing porosity coefficient, mode number, volume fraction, types of reinforcement, and slenderness ratio. A detailed and delineated parametric study is accomplished to spotlight and emphasize the influence and leverage of porosity parameters on the structural performance of porous beams.

2 Functionally graded carbon nanotube-reinforced composites porous beams

The CNTRC porous beam is composed of a polymer matrix mixed with SWCNTs. Fig. 1 (a) shows a CNTRC porous beam, having length (L) and thickness (h).

This study considers and appraises dissonant reinforcement patterns over the cross-sections, as indicated in Fig. 1 (b). Besides, the rule of the mixture can be used to determine the effective mechanical properties of CNTRC porous beams [41]:

$$E_{11} = \eta_1 V_{\mathrm{CNT}} E_{11}^{\mathrm{CNT}} + V_p E_p, \tag{1}$$

$$\frac{\eta_2}{E_{22}} = \frac{V_{\mathrm{CNT}}}{E_{22}^{\mathrm{CNT}}} + \frac{V_p}{E_p}, \tag{2}$$

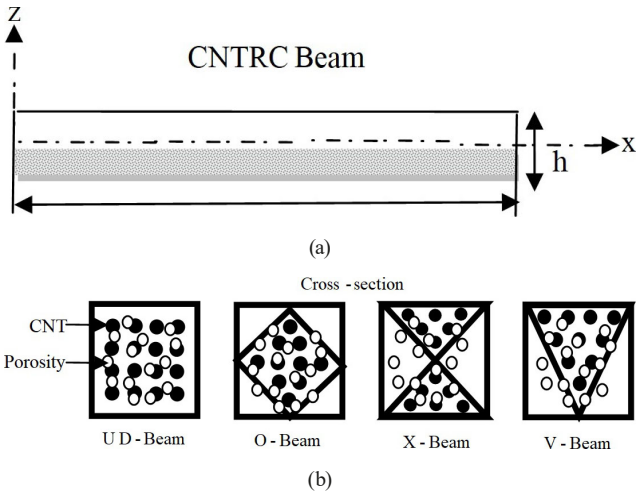

Fig. 1 (a) geometry of a CNTRC beam and (b) cross sections of different patterns of reinforcement

$$\frac{\eta_3}{G_{12}} = \frac{V_{\mathrm{CNT}}}{G_{12}^{\mathrm{CNT}}} + \frac{V_p}{G_p}, \tag{3}$$

where: E_{11}^{CNT}, E_{22}, E_p and G_{12}^{CNT}, G_p are Young's modulus and shear modulus of SWCNT and the polymer matrix, respectively.

The Young's modulus of the polymer matrix, under porosity, which may be a function of porosity change, is defined by Kováčik [42]:

$$E_p = E_0^p \left(1 - P/P_c\right), \tag{4}$$

where E_p is the effective Young's modulus of the porous matrix with porosity P, E_0^p is Young's modulus of the matrix without porosity, P_c represents and constitutes the porosity at which the effective Young's modulus becomes zero. In experimental works, either (P_c = 1) is preferably used. Other properties in terms of mass density (ρ) and Poisson's ratio (v) can be defined as [41]:

$$v = V_{\mathrm{CNT}} v_{12}^{\mathrm{CNT}} + V_p \rho^p, \tag{5}$$

$$\rho = V_{\mathrm{CNT}} \rho^{\mathrm{CNT}} + V_p \rho^p. \tag{6}$$

Presuming that V_{CNT} and V_p are the volume fractions of the CNT and porous matrix, respectively. The mass density may also be a function of porosity change [42].

$$\rho^p = \rho_0^p \left(1 - P/P_c\right). \tag{7}$$

Below are the mathematical functions required to introduce various patterns of carbon nanotube reinforcement distributed within the beam's cross-sections, as depicted in Fig. 1 (b) [43]:

$$\text{UD-Beam: } V_{\mathrm{CNT}} = V_{\mathrm{CNT}}^*, \tag{8}$$

$$\text{O-Beam: } V_{\mathrm{CNT}} = 2\left(1 - 2\frac{|z|}{h}\right) V_{\mathrm{CNT}}^*, \tag{9}$$

$$\text{X-Beam: } V_{\mathrm{CNT}} = 4\frac{|z|}{h} V_{\mathrm{CNT}}^*. \tag{10}$$

With the supposition, V_{CNT}^* the considered volume fraction of CNTs is determined and purposeful from Eq. (11) [42]:

$$V_{\mathrm{CNT}}^* = \frac{W_{\mathrm{CNT}}}{W_{\mathrm{CNT}} + \left(\rho^{\mathrm{CNT}}/\rho^m\right)\left(1 - W_{\mathrm{CNT}}\right)}. \tag{11}$$

The symbol W_{CNT} denotes the mass fraction of carbon nanotubes (CNTs). Equations (5) and (6) shows that the O-, X-, and V-Beams represent examples of FG beams, where the material composition changes continuously throughout the thickness of the beam. On the other hand, the UD-Beam has a uniform distribution of CNT reinforcement. In this work, the CNT efficiency parameters (η_i) associated with the considered volume fraction ($V_{\mathrm{CNT}} V_{\mathrm{CNT}}^*$) are: η_1 = 1.2833 and $\eta_2 = \eta_3$ = 1.0566 for the case of V_{CNT}^* = 0.12, for the case of V_{CNT}^* = 0.28 [44].

3 Theory and formulations

3.1 Displacement field of refined beam theory

The displacement field of trigonometric refined beam theory with only three unknowns is used in the present theory and is defined as [43]:

$$u(x,z) = u_0(x) - z\frac{\partial w_b}{\partial x} - f(z)\frac{\partial w_s}{\partial x}, \tag{12}$$

$$w(x,z) = w_b(x) + w_s(x), \tag{13}$$

where u_0 represents the axial displacement while w_s and w_b represent the transverse shift components of shear and bending, respectively, along the mid-plane of the beam. In this work, the shape function $f(z)$ is selected based on a trigonometric function [43].

$$f(z) = z - \left(h \sinh\left(\frac{z}{h}\right) e^{-2\left(\frac{z}{h}\right)^2}\right) \tag{14}$$

In terms of the plane and transverse strains, the relationship between linear strain and displacement can be expressed as:

$$\varepsilon_x = \frac{\partial u_0}{\partial x} + z\frac{\partial^2 w_b}{\partial x^2} + f(z)\frac{\partial^2 w_s}{\partial x^2}, \tag{15}$$

$$y_{xz} = g(z)\frac{\partial w_s}{\partial x}, \tag{16}$$

where:

$$g(z) = 1 - f'(z) \text{ and } f'(z) = \frac{df(z)}{d(z)}. \tag{17}$$

Assuming that the material of the CNTRC beam follows Hooke's law, the stress in the beam can be calculated [41]:

$$\sigma_x = Q_{11}(z)\varepsilon_x \text{ and } \tau_{xz} = Q_{55}(z) y_{xz}, \tag{18}$$

$$Q_{55}(z) = G_{12}(z) \text{ and } Q_{11}(z) = \frac{E_{11}(z)}{1 - v^2}. \tag{19}$$

3. 2 Hamilton's principle

The virtual work principle is used herein to determine and ascertain stability equations as follows in Eq. (20) [45]:

$$\left(\delta U+\delta V\right)=0. \tag{20}$$

Assuming that δU represents the virtual variation of strain energy and δV represents the virtual variation of potential energy, the variation of beam strain energy can be expressed as [46]:

$$\begin{aligned}\delta U&=\int_0^L\int_{-h/2}^{h/2}\left(\sigma_x\delta\varepsilon_x+\tau_{xz}\delta\gamma_{xz}\right)dzdx\\&=\int_0^L\begin{pmatrix}N\dfrac{d\delta u_0}{dx}-M_b\dfrac{d^2\delta w_b}{dx^2}\\-M_s\dfrac{d^2\delta w_s}{dx^2}+Q\dfrac{d\delta w_b}{dx}\end{pmatrix},\end{aligned} \tag{21}$$

where N, M_b, M_s and Q are the stress resultants defined as:

$$\begin{aligned}&\left(N,M_b,M_s\right)=\int_{-h/2}^{h/2}\left(1,z,f\left(z\right)\right)\sigma_x dz\\&\text{and }Q=\int_{-h/2}^{h/2}g\left(z\right)\tau_{xz}dz.\end{aligned} \tag{22}$$

The variation of the potential energy done by applied forces can be stated as [47]:

$$\delta V=-\int_0^L\left[N_{x0}\frac{d\left(w_b+w_s\right)d\left(\delta w_b+\delta w_s\right)}{dx}\right]dx. \tag{23}$$

To obtain the CNTRC beam's motion equations, we substitute the expressions δU, δV from Eqs. (15)–(17), (20), and (22) into Eq. (14). This requires integrating by parts with respect to both space and time variables and collecting the coefficients of δu_0, δw_b and δw_s:

$$\delta u_0:\frac{dN}{dx}=0, \tag{24}$$

$$\delta w_b:\frac{d^2M_b}{dx^2}+N_{x0}\frac{d^2\left(w_b+w_s\right)}{dx^2}=0, \tag{25}$$

$$\delta w_s:\frac{d^2M_s}{dx^2}+\frac{dQ}{dx}+N_{x0}\frac{d^2\left(w_b+w_s\right)}{dx^2}=0. \tag{26}$$

By substituting Eq. (12) into Eq. (13) and subsequently substituting the results into Eqs. (18) and (19), the constitutive equations for the stress resultants can be derived:

$$N=A_{11}\frac{du_0}{dx}-B_{11}\frac{d^2w_b}{dx^2}-B_{11}^s\frac{d^2w_s}{dx^2}, \tag{27}$$

$$M_b=B_{11}\frac{du_0}{dx}-D_{11}\frac{d^2w_b}{dx^2}-D_{11}^s\frac{d^2w_s}{dx^2}, \tag{28}$$

$$M_s=B_{11}^s\frac{du_0}{dx}-D_{11}^s\frac{d^2w_b}{dx^2}-H_{11}^s\frac{d^2w_s}{dx^2}, \tag{29}$$

$$Q=A_{55}^s\frac{dw_s}{dx}, \tag{30}$$

where A_{11}, B_{11}, etc., denote the beam stiffness and can be determined by:

$$\begin{aligned}&\left(A_{11},B_{11},D_{11},B_{11}^s,D_{11}^s,H_{11}^s\right)\\&=\int_{-h/2}^{h/2}\left(1,z,z^2,f\left(z\right),z\,f\left(z\right),f^2\left(z\right)\right)dz,\end{aligned} \tag{31}$$

where:

$$A_{55}^s=\int_{-h/2}^{h/2}Q_{55}\left[g\left(z\right)\right]^2dz. \tag{32}$$

Using Eqs. (27)–(30) and Eqs. (24)–(26), Eqs. (24)–(26) can be found in terms of displacements (du_0, dw_b, dw_s):

$$A_{11}\frac{\partial^2u_0}{dx^2}-B_{11}\frac{\partial^3w_b}{dx^3}-B_{11}^s\frac{\partial^3w_s}{dx^3}=0, \tag{33}$$

$$\begin{aligned}&B_{11}\frac{\partial^3u_0}{\partial x^3}-D_{11}\frac{\partial^4w_b}{\partial x^4}-D_{11}^s\frac{\partial^4w_s}{\partial x^4}\\&+N_{x0}\frac{d^2\left(w_b+w_s\right)}{dx^2}=0,\end{aligned} \tag{34}$$

$$\begin{aligned}&B_{11}^s\frac{\partial^3u_0}{\partial x^3}-D_{11}^s\frac{\partial^4w_b}{\partial x^4}-H_{11}^s\frac{\partial^4w_s}{\partial x^4}\\&+A_{55}\frac{\partial^2w_s}{\partial x^2}+N_{x0}\frac{d^2\left(w_b+w_s\right)}{dx^2}=0.\end{aligned} \tag{35}$$

3.3 Solution methodology

Since the simplicity of the solution method is desirable in various applications, the obtained differential equations can be solved analytically with the Navier method of simply supported CNTRC beam. It is assumed that the solution is in a specific form [43]:

$$\begin{Bmatrix}u_0\\w_b\\w_s\end{Bmatrix}=\sum_{m=1}^{\infty}\begin{Bmatrix}U_m\cos\left(\lambda x\right)\\W_{bm}\sin\left(\lambda x\right)\\W_{sm}\sin\left(\lambda x\right)\end{Bmatrix}, \tag{36}$$

with:

$$\lambda=m\pi/L, \tag{37}$$

where U_m, W_{bm} and W_{sm} are arbitrary parameters to be determined, Substituting the expansions of u_0, w_b, w_s, and q from Eqs. (36) and (37) into the equations of motion Eqs. (33)–(35), the analytical solutions can be obtained from the succeeding equations:

$$\left(\begin{bmatrix} S_{11} & S_{12} & S_{13} \\ S_{12} & S_{22} & S_{23} \\ S_{13} & S_{23} & S_{33} \end{bmatrix}\right)\begin{Bmatrix} u_m \\ w_{bm} \\ w_{sm} \end{Bmatrix} = \begin{Bmatrix} 0 \\ 0 \\ 0 \end{Bmatrix}, \tag{38}$$

$$\begin{aligned} &S_{11} = A_{11}\lambda^2,\ S_{12} = -B_{11}\lambda, \\ &S_{13} = -B^s_{11}\lambda,\ S_{22} = D_{11}\lambda^4 + N_{cr}\lambda^2, \\ &S_{23} = D^s_{11}\lambda^4 + N_{cr}\lambda^2, \\ &S_{33} = H^s_{11}\lambda^2 + A^s_{55}\lambda^2 + N_{cr}\lambda^2. \end{aligned} \tag{39}$$

4 Numerical results and discussion

This section represents the numerical results of the buckling behaviors of CNTRC beams. The material characteristics of CNTRC porous beams at ambient temperature employed through this work areas follows. Polymethyl methacrylate (PMMA) is assumed to be the matrix that the material properties are set as follows: v^p = 0.3, ρ^p = 1190 Kg/m^3 and E^p = 2.5 GPa. In addition, the armchair (10, 10) SWCNTs are used as reinforcement with the materials properties [44]: v^{CNT} = 0.19, ρ^{CNT} = 1400 Kg/m^3, $E^{\mathrm{CNT}}_{11} = 600$ GPa, $E^{\mathrm{CNT}}_{22} = 10$ GPa and $G^{\mathrm{CNT}}_{12} = 17.2$ GPa.

The dimensionless critical buckling loads considered in this analysis can be represented as follows [43]:

$$\bar{N} = \frac{N_{cr}}{A_{110}}. \tag{40}$$

The current section discusses and argues the numerical results of the buckling analysis of CNTRC beams.

In an attempt to validate the present work, critical buckling loads of a nanocomposite beam reinforced by CNTs are studied, neglecting porosity. In this case, the obtained results of dimensionless critical buckling loads based on the refined trigonometric beam theory are illustrated in Table 1, which agrees with the reference mentioned.

In order to indicate the influence of porosity on the critical buckling loads of reinforced beams, different distributions of CNTs are considered. With different mode numbers, the dimensionless critical buckling loads ($\bar{N}$) of reinforced porous beams for UD-CNT and various FG-CNT reinforcements under axial and biaxial compressive loads are presented in Table 2. The critical buckling loads are expected to increase with the mode number for all reinforcement types. This increase in critical buckling loads for higher modes is attributed to the configuration of a small wavelength. On the other hand, the dimensionless critical buckling loads decrease if the porosity increases for all mode numbers.

It is known that increasing the carbon nanotube volume fraction can make the beam stiffer. This remark was expected and demonstrated in Table 3, which represents the increases in the critical buckling loads with increasing carbon nanotube volume fraction for all reinforcement types of the porous beam. According to the results, it is clear that the X-CNT reinforced beam has higher dimensionless critical buckling loads than those of other reinforcement types for every case of porosity and carbon nanotube volume fraction.

Among the results of the current study, Table 4 depicts the dimensionless critical buckling loads of a reinforced (O-CNT) porous beam for various values of porosity and aspect ratio (L/h). It is observed that when the length of the beam increases for high values of aspect ratio, the critical buckling loads decrease. It is concluded that the augmentation or diminution of dimensionless critical loads is allotted to the beam's length and width variations. When the length of the beam decreases, it requires a high load to buckle. Furthermore, the reinforced beam without porosity has a higher resistance against buckling than the porous beam because the latter is affected by increasing porosity. It is concluded that the increase of pores in the polymer matrix makes the beam less rigid.

Fig. 2 is plotted to clearly show the influence of porosity and aspect ratio (L/h) on the dimensionless critical

Table 1 Comparisons of dimensionless critical buckling loads ($\bar{N}$) of CNTRC beam (L/h = 15, V^*_{CNT} = 0.12)

Source	UD-CNT	O-CNT	X-CNT
Yas and Samadi [45]	0.0986	0.0588	0.1288
Wattanasakulpong and Ungbhakorn (TSDT) [42]	0.0984	0.0576	0.1289
Wattanasakulpong and Ungbhakorn (ESDT) [42]	0.0987	0.0574	0.1295
Wattanasakulpong and Ungbhakorn (HSDT) [42]	0.0984	0.0576	0.1288
Tagrara et al. [44]	0.0985	0.0575	0.1291
Present	0.0985	0.0575	0.1292

Table 2 Critical buckling loads ($\bar{N}$) of CNTRC porous beam for different mode number (L/h = 10, V^*_{CNT} = 0.12)

Mode	P (%)	UD-CNT	X-CNT	O-CNT
1	0	0.1646	0.2008	0.1052
	0.005	0.1543	0.1861	0.1000
	0.01	0.1425	0.1697	0.0940
	0.02	0.1129	0.1301	0.0780
2	0	0.2826	0.3115	0.2118
	0.005	0.2560	0.2806	0.1935
	0.01	0.2279	0.2484	0.1737
	0.02	0.1666	0.1797	0.1287
3	0	0.3417	0.3680	0.2662
	0.005	0.3078	0.3311	0.2396
	0.01	0.2730	0.2934	0.2118
	0.02	0.2001	0.2157	0.1525

Table 3 Critical buckling loads ($\bar{N}$) of CNTRC porous beam for different nanotube volume fraction (L/h = 10)

V^*_{CNT}	P (%)	UD-CNT	X-CNT	O-CNT
0.12	0	0.1646	0.2008	0.1052
	0.005	0.1543	0.1861	0.1000
	0.01	0.1425	0.1697	0.0940
	0.02	0.1129	0.1301	0.0780
0.17	0	0.2581	0.3161	0.1624
	0.005	0.2433	0.2943	0.1555
	0.01	0.2261	0.2696	0.1473
	0.02	0.1819	0.2091	0.1248
0.28	0	0.3562	0.4106	0.2414
	0.005	0.3328	0.3784	0.2302
	0.01	0.3062	0.3428	0.2170
	0.02	0.2400	0.2591	0.1811

Table 4 Effect of aspect ratio L/h and porosity on the dimensionless critical buckling loads of reinforced O-CNT porous beam (V^*_{CNT} = 0.12)

L/h	P = 0%	P = 0.005%	P = 0.01%	P = 0.02%
1	0.4793	0.4407	0.4019	0.3237
2	0.3271	0.2936	0.2596	0.1896
3	0.2787	0.2503	0.2210	0.1588
4	0.2431	0.2200	0.1956	0.1420
5	0.2118	0.1935	0.1737	0.1287
6	0.1839	0.1697	0.1539	0.1168
7	0.1595	0.1485	0.1361	0.1058
8	0.1384	0.1299	0.1202	0.0957
9	0.1205	0.1138	0.1062	0.0864
10	0.1052	0.1000	0.0940	0.0780

buckling loads of reinforced porous beams for O-CNT and X-CNT distributions. The aspect ratio (L/h) has been varied between 3 and 30. On the other hand, four values were used to clearly show the effect of porosity (0, 0.005, 0.01 and 0.02). The dimensionless critical buckling loads ($\bar{N}$) are inversely related to the slenderness ratio (L/h) and porosity. The dimensionless critical buckling loads decrease by converging to a certain value with the increase of aspect ratio, and the lowest values of critical loads ($\bar{N}$) have prevailed for porous beams with P = 0.02%, and this is for both types of beams (X-beam and O-beam). Comparing the results, it can be seen that the dimensionless critical buckling loads

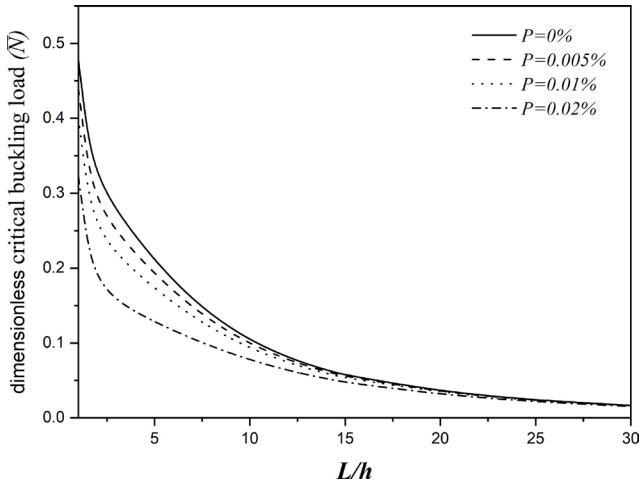

(a)

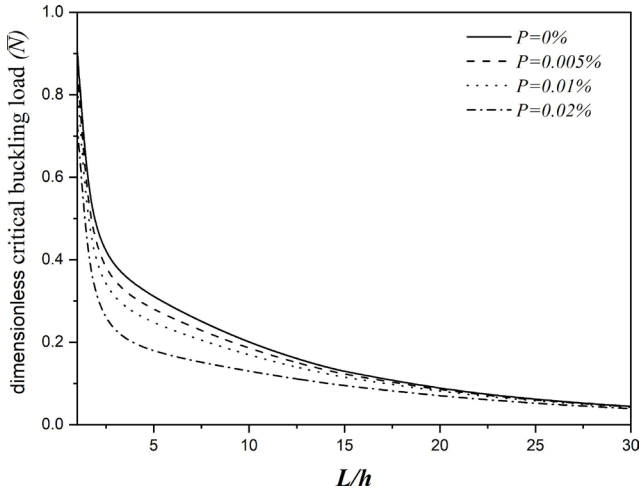

(b)

Fig. 2 Effect of aspect ratio L/h and porosity on the critical buckling loads of reinforced perfect and porous square CNT beams (V^*_{CNT} = 0.12): (a) O-beam and (b) X-beam

decrease with the increase in porosity. The decrease in critical loads is attributed to the porosity's effect on the porous beam's rigidity.

It is readily seen in the current study that the rigidity of reinforced porous beam is affected by the existence of porosity, which is demonstrated in (Fig. 3) with aspect ratio (a/h = 10) and various volume fractions with uniformly and non-uniformly distributed nanotubes in the beams. It is worth noting in the figure that the critical buckling loads of reinforced porous beams decrease if the porosity increases for all three studied cases of reinforcement type. It is also concluded that the X-CNT type has the highest critical buckling loads in the studied cases. Therefore, it has the highest stiffness. The highest critical buckling loads estimated in the X-CNT case are attributed to the carbon nanotube concentration at the bottom and top face of the beam.

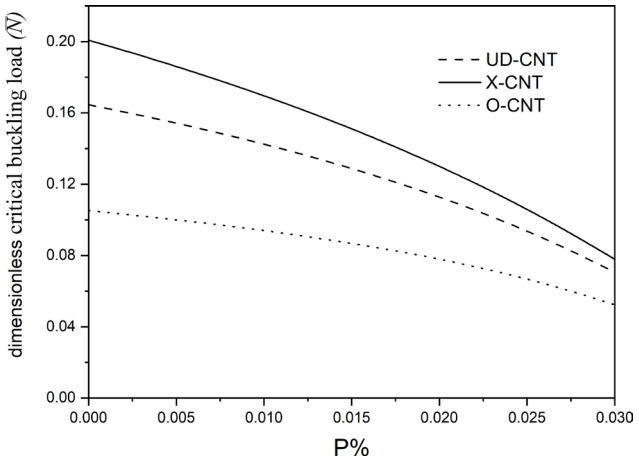

(a)

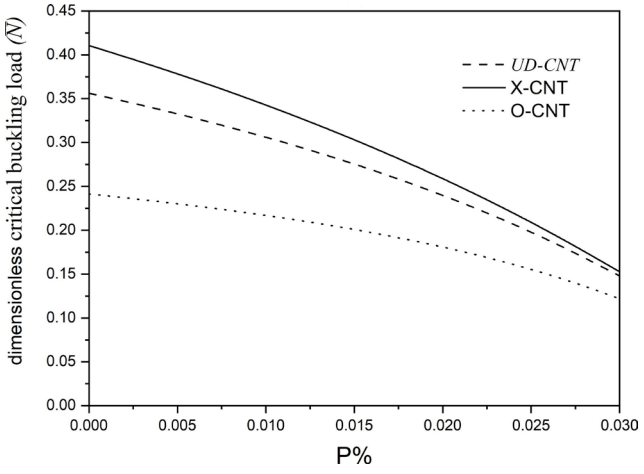

(b)

Fig. 3 Effect of porosity on the critical buckling loads of reinforced porous beam for various reinforcement types: (a) V^*_{CNT} = 0.12; (b) V^*_{CNT} = 0.28

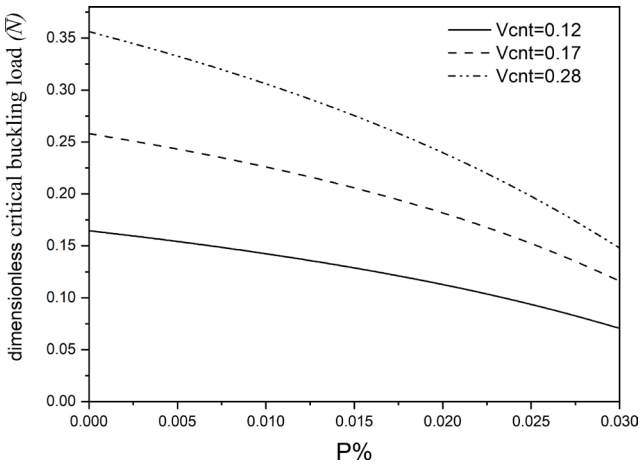

Fig. 4 Effect of porosity on the critical buckling loads of reinforced porous beam for various carbon nanotube volume fractions (V^*_{CNT})

One of the goals of this study is to investigate the effects of uniformly and non-uniformly distributed nanotubes in beams with and without porosity. As may be observed

in Fig. 4, the variation between the distributed nanotube cases is very important without porosity and then decreases with their increase. This is due to the effect of porosity on the rigidity of the beam. Increasing the volume fraction (V_{CNT}) of carbon nanotubes can be used to compensate for the decrease in rigidity. This analysis is very clear in Fig. 4. The critical buckling load range increases as the volume fraction of carbon nanotubes increases. It is concluded that increasing the carbon nanotube volume fraction can make the beam stiffer, which requires a greater critical buckling load.

5 Conclusions

In this research, the critical buckling loads of reinforced porous beams are computed numerically using the trigonometric refined beam theory with only three unknowns mixed with Hamilton's principle. The nanocomposite comprised a polymer matrix and CNTs incorporated with the mixture rule. The influence of porosity and different parameters on the critical buckling loads of reinforced porous beams is analyzed and discussed. Firstly, the accuracy of the present model is confirmed by comparing the current results with those obtained by other theories existing in the literature. Subsequent understandings related to the parametric analysis, such as porosity, volume fraction, aspect ratios, and types of reinforcement, are discussed in point-wise form in the following lines:

- It is found that the critical buckling loads of reinforced porous beams decrease by increasing the porosity in the polymer beam. This is due to the effect of porosity on the rigidity of the beam.
- The results obtained from the analysis of critical buckling loads indicated that the X-CNT reinforced beam has a high resistance against buckling compared to other reinforcement types because of the nanotube concentration at the top and bottom faces of the beam.
- As the aspect ratio increases, the critical buckling loads decrease.
- It is concluded that increasing the carbon nanotube volume fraction can make the beam stiffer, which requires a greater critical buckling load.

Nomenclature

MD	Simulation method
CNTs	Carbon nanotubes
SWCNTs	Single-walled carbon nanotubes
CNTRCs	Carbon nanotube-reinforced composites
L	Length of the beam
h	Thickness of the beam
E_{11}^{CNT}	Axial Young's modulus of SWCNT
E_{22}	Transversal Young's modulus of SWCNT
E_p	Young's modulus of the polymer matrix
G_{12}^{CNT}	Shear modulus of SWCNT
G_p	Shear modulus of the polymer matrix
E_0^p	Young's modulus of the matrix without porosity
P	The porosity
V_{CNT}	Volume fractions of the CNT
V_p	Volume fractions of the porous matrix
η_i	Efficiency parameters
u_0	Axial displacement
w_s, w_b	Transverse shift components of shear and bending
δU	Virtual strain energy
δV	Virtual potential energy
N, M_b, M_s, Q	The stress resultants
U_m, W_{bm}, W_{sm}	Arbitrary parameters
N_{cr}	Critical buckling loads
$f(z)$	Trigonometric function.

Acknowledgments

The Authors extend their appreciation to the Deanship Scientific Research at King Khalid University for funding this work through large group Research Project under grant number: RGP2/463/44.

Declarations

Conflict of interest: All authors declare that they have no conflicts of interest.

Ethical statement: Authors state that the research was conducted according to ethical standards.

References

[1] Rachedi, M. A., Benyoucef, S., Bouhadra, A., Bouiadjra, R. B., Sekkal, M., Benachour, A. "Impact of the homogenization models on the thermoelastic response of FG plates on variable elastic foundation", Geomechanics and Engineering, 22(1), pp. 65–80, 2020. https://doi.org/10.12989/gae.2020.22.1.065

[2] Timesli, A. "Buckling analysis of double walled carbon nanotubes embedded in Kerr elastic medium under axial compression using the nonlocal Donnell shell theory", Advances in Nano Research, 9(2), pp. 69–83, 2020. https://doi.org/10.12989/anr.2020.9.2.069

[3] Sobamowo, M. G. "Nonlinear thermal and flow-induced vibration analysis of fluid-conveying carbon nanotube resting on Winkler and Pasternak foundations", Thermal Science and Engineering Progress, 4, pp. 133–149, 2017. https://doi.org/10.1016/j.tsep.2017.08.005

[4] Sui, G., Liu, D., Liu, Y., Ji, W., Zhang, Q., Fu, Q. "The dispersion of CNT in TPU matrix with different preparation methods: solution mixing vs melt mixing", Polymer, 182, 121838, 2019. https://doi.org/10.1016/j.polymer.2019.121838

[5] Lahelin, M., Annala, M., Nykänen, A., Ruokolainen, J., Seppälä, J. "In situ polymerized nanocomposites: Polystyrene/CNT and Poly (methyl methacrylate)/CNT composites", Composites Science and Technology, 71(6), pp. 900–907, 2011. https://doi.org/10.1016/j.compscitech.2011.02.005

[6] Yeo, L. Y., Friend, J. R. "Electrospinning carbon nanotube polymer composite nanofibers", Journal of Experimental Nanoscience, 1(2), pp. 177–209, 2006. https://doi.org/10.1080/17458080600670015

[7] Olek, M., Ostrander, J., Jurga, S., Möhwald, H., Kotov, N., Kempa, K., Giersig, M. "Assembled Composites from Multiwall Carbon Nanotubes with Different Morphologies", Nano Letters, 4(10), pp. 1889–1895, 2004. https://doi.org/10.1021/nl048950w

[8] Ajayan, P. M., Stephan, O., Colliex, C., Trauth, D. "Aligned carbon nanotube arrays formed by cutting a polymer resin—nanotube composite", Science, 265(5176), pp. 1212–1214, 1994. https://doi.org/10.1126/science.265.5176.1212

[9] Tayeb, T. S., Zidour, M., Bensattalah, T., Heireche, H., Benahmed, A., Bedia, E. A. A. "Mechanical buckling of FG-CNTs reinforced composite plate with parabolic distribution using Hamilton's energy principle", Advances in Nano Research, 8(2), pp. 135–148, 2020. https://doi.org/10.12989/anr.2020.8.2.135

[10] Karami, B., Shahsavari, D., Janghorban, M. "A comprehensive analytical study on functionally graded carbon nanotube-reinforced composite plates", Aerospace Science and Technology, 82–83, pp. 499–512, 2018. https://doi.org/10.1016/j.ast.2018.10.001

[11] Abdelmalek, A., Bouazza, M., Zidour, M., Benseddiq, N. "Hygrothermal Effects on the Free Vibration Behavior of Composite Plate Using nth-Order Shear Deformation Theory: a Micromechanical Approach", Iranian Journal of Science and Technology, Transactions of Mechanical Engineering, 43(1), pp. 61–73, 2019. https://doi.org/10.1007/s40997-017-0140-y

[12] Shokrieh, M. M., Rafiee, R. "A review of the mechanical properties of isolated carbon nanotubes and carbon nanotube composites", Mechanics of Composite Materials, 46(2), pp. 155–172, 2010. https://doi.org/10.1007/s11029-010-9135-0

[13] Srivastava, R. K., Vemuru, V. S. M., Zeng, Y., Vajtai, R., Nagarajaiah, S., Ajayan, P. M., Srivastava, A. "The strain sensing and thermal–mechanical behavior of flexible multi-walled carbon nanotube/polystyrene composite films", Carbon, 49(12), pp. 3928–3936, 2011. https://doi.org/10.1016/j.carbon.2011.05.031

[14] Alibeigloo, A. "Three-dimensional thermoelasticity solution of functionally graded carbon nanotube reinforced composite plate embedded in piezoelectric sensor and actuator layers", Composite Structures, 118, pp. 482–495, 2014. https://doi.org/10.1016/j.compstruct.2014.08.004

[15] Hamidi, A., Zidour, M., Bouakkaz, K., Bensattalah, T. "Thermal and Small-Scale Effects on Vibration of Embedded Armchair Single-Walled Carbon Nanotubes", Journal of Nano Research, 51, pp. 24–38, 2018. https://doi.org/10.4028/www.scientific.net/JNanoR.51.24

[16] Esen, I., Abdelrhmaan, A. A. Eltaher, M. A. "Free vibration and buckling stability of FG nanobeams exposed to magnetic and thermal fields", Engineering with Computers, 38(4), pp. 3463–3482, 2022. https://doi.org/10.1007/s00366-021-01389-5

[17] Aslam, M. M.-A., Kuo, H.-W., Den, W., Usman, M., Sultan, M., Ashraf, H. "Functionalized Carbon Nanotubes (CNTs) for Water and Wastewater Treatment: Preparation to Application", Sustainability, 13(10), 5717, 2021. https://doi.org/10.3390/su13105717

[18] Dilimon, V. S., Shibli, S. M. A. "Application of Surface Modified Carbon Nanotubes in Fuel Cells", In: Aslam, J., Hussain, C. M., Aslam, R. (eds.) Surface Modified Carbon Nanotubes Volume 2: Industrial Applications, ACS Publications Series, 2022, pp. 121–150. ISBN 9780841297470 https://doi.org/10.1021/bk-2022-1425.ch006

[19] Fu, S.-Y., Lauke, B., Mäder, E., Yue, C.-Y., Hu, X. "Tensile properties of short-glass-fiber-and short-carbon-fiber-reinforced polypropylene composites", Composites Part A: Applied Science and Manufacturing, 31(10), pp. 1117–1125, 2000. https://doi.org/10.1016/S1359-835X(00)00068-3

[20] Joshi, S. V., Drzal, L. T., Mohanty, A. K., Arora, S. "Are natural fiber composites environmentally superior to glass fiber reinforced composites?", Composites Part A: Applied science and manufacturing, 35(3), pp. 371–376, 2004. https://doi.org/10.1016/j.compositesa.2003.09.016

[21] Wang, H. W., Zhou, H. W., Gui, L. L., Ji, H. W., Zhang, X. C. "Analysis of effect of fiber orientation on Young's modulus for unidirectional fiber reinforced composites", Composites Part B: Engineering, 56, pp. 733–739, 2014. https://doi.org/10.1016/j.compositesb.2013.09.020

[22] Yaylacı, M., Abanoz, M., Yaylacı, E. U., Ölmez, H., Sekban, D. M., Birinci, A. "Evaluation of the contact problem of functionally graded layer resting on rigid foundation pressed via rigid punch by analytical and numerical (FEM and MLP) methods", Archive of Applied Mechanics, 92(6), pp. 1953–1971, 2022. https://doi.org/10.1007/s00419-022-02159-5

[23] Yaylacı, M., Şabano, B. Ş., Özdemir, M. E., Birinci, A. "Solving the contact problem of functionally graded layers resting on a HP and pressed with a uniformly distributed load by analytical and numerical methods", Structural Engineering and Mechanics, 82(3), pp. 401–416, 2022. https://doi.org/10.12989/sem.2022.82.3.401

[24] Adıyaman, G., Öner, E., Yaylacı, M., Birinci, A. "A study on the contact problem of a layer consisting of functionally graded material (FGM) in the presence of body force", Journal of Mechanics of Materials and Structures, 18(1), pp. 125–141, 2023. https://doi.org/10.2140/jomms.2023.18.125

[25] Yaylacı, M., Abanoz, M., Yaylacı, E. U., Olmez, H., Sekban, D. M., Birinci, A. "The contact problem of the functionally graded layer resting on rigid foundation pressed via rigid punch", Steel and Composite Structures, 43(5), pp. 661–672, 2022. https://doi.org/10.12989/scs.2022.43.5.661

[26] Yaylacı, E. U., Yaylaci, M., Abushattal, A. "Application of artificial neural networks in the analysis of the continuous contact problem", Structural Engineering and Mechanics, 84(1), pp. 35–48, 2002. https://doi.org/10.12989/sem.2022.84.1.035

[27] Özdemir, M. E., Yaylac, M. "Research of the impact of material and flow properties on fluid-structure interaction in cage systems", Wind and Structures, 36(1), pp. 31–40, 2023. https://doi.org/10.12989/was.2023.36.1.031

[28] Yaylacı, M. "The investigation crack problem through numerical analysis", Structural Engineering and Mechanics, 57(6), pp. 1143–1156, 2016. https://doi.org/10.12989/sem.2016.57.6.1143

[29] Yaylacı, M., Uzun Yaylacı, E., Ozdemir, M. E., Ay, S., Ozturk, S. "Implementation of finite element and artificial neural network methods to analyze the contact problem of a functionally graded layer containing crack", Steel and Composite Structures, 45(4), pp. 501–511, 2022. https://doi.org/10.12989/scs.2022.45.4.501

[30] Yaylaci, M., Yayli, M., Yaylaci, E. U., Olmez, H., Birinci, A. "Analyzing the contact problem of a functionally graded layer resting on an elastic half plane with theory of elasticity, finite element method and multilayer perceptron", Structural Engineering and Mechanics, 78(5), pp. 585–597, 2021. https://doi.org/10.12989/sem.2021.78.5.585

[31] Öner, E., Şengül Şabano, B., Uzun Yaylacı, E., Adıyaman, G., Yaylacı, M., Birinci, A. "On the plane receding contact between two functionally graded layers using computational, finite element and artificial neural network methods", ZAMM-Journal of Applied Mathematics and Mechanics/Zeitschrift für Angewandte Mathematik und Mechanik, 102(2), e202100287, 2022. https://doi.org/10.1002/zamm.202100287

[32] Yaylaci, M. "Simulate of edge and an internal crack problem and estimation of stress intensity factor through finite element method", Advances in Nano Research, 12(4), pp. 405–414, 2022. https://doi.org/10.12989/anr.2022.12.4.405

[33] Sisodia, S., Gamstedt, E. K., Edgren, F., Varna, J. "Effects of voids on quasi-static and tension fatigue behaviour of carbon-fibre composite laminates", Journal of Composite Materials, 49(17), pp. 2137–2148, 2015. https://doi.org/10.1177/0021998314541993

[34] Turan, M., Uzun Yaylacı, E., Yaylacı, M. "Free vibration and buckling of functionally graded porous beams using analytical, finite element, and artificial neural network methods", Archive of Applied Mechanics, 93(4), pp. 1351–1372, 2023. https://doi.org/10.1007/s00419-022-02332-w

[35] Liu, L., Zhang, B.M., Wang, D.-F., Wu, Z.-J. "Effects of cure cycles on void content and mechanical properties of composite laminates", Composite Structures, 73(3), pp. 303–309, 2006. https://doi.org/10.1016/j.compstruct.2005.02.001

[36] Ghiorse, S. R. "Effect of void content on the mechanical properties of carbon/epoxy laminates", SAMPE Quarterly, 24(2), pp. 54–59, 1993.

[37] Wan, H., Delale, F., Shen, L. "Effect of CNT length and CNT-matrix interphase in carbon nanotube (CNT) reinforced composites", Mechanics Research Communications, 32(5), pp. 481–489, 2005. https://doi.org/10.1016/j.mechrescom.2004.10.011

[38] Faleh, N. M., Ahmed, R. A., Fenjan, R. M. "On vibrations of porous FG nanoshells", International Journal of Engineering Science, 133, pp. 1–14, 2018. https://doi.org/10.1016/j.ijengsci.2018.08.007

[39] Vinyas, M. "On frequency response of porous functionally graded magneto-electro-elastic circular and annular plates with different electro-magnetic conditions using HSDT", Composite Structures, 240, 112044, 2020. https://doi.org/10.1016/j.compstruct.2020.112044

[40] Yaylacı, M., Yaylacı, E. U., Ozdemir, M. E., Oztürk, Ş., Sesli, H. "Vibration and buckling analyses of FGM beam with edge crack: Finite element and multilayer perceptron methods", Steel and Composite Structures, 46(4), pp. 565–575, 2023. https://doi.org/10.12989/scs.2023.46.4.565

[41] Wattanasakulpong, N., Ungbhakorn, V. "Analytical solutions for bending, buckling and vibration responses of carbon nanotube-reinforced composite beams resting on elastic foundation", Computational Materials Science, 71, pp. 201–208, 2013. https://doi.org/10.1016/j.commatsci.2013.01.028

[42] Kováčik, J. "Correlation between Young's modulus and porosity in porous materials", Journal of Materials Science Letters, 18(13), pp. 1007–1010, 1999. https://doi.org/10.1023/A:1006669914946

[43] Tagrara, S. H., Benachour, A., Bouiadjra, M. B., Tounsi, A. "On bending, buckling and vibration responses of functionally graded carbon nanotube-reinforced composite beams", Steel and Composite Structures, 19(5), pp. 1259–1277, 2015. https://doi.org/10.12989/scs.2015.19.5.1259

[44] Yas, M. H., Samadi, N. "Free vibrations and buckling analysis of carbon nanotube-reinforced composite Timoshenko beams on elastic foundation", International Journal of Pressure Vessels and Piping, 98, pp. 119–128, 2012.
https://doi.org/10.1016/j.ijpvp.2012.07.012

[45] Talha, M., Singh, B. N. "Static response and free vibration analysis of FGM plates using higher order shear deformation theory", Applied Mathematical Modelling, 34(12), pp. 3991–4011, 2010.
https://doi.org/10.1016/j.apm.2010.03.034

[46] Batou, B., Nebab, M., Bennai, R., Atmane, H. A., Tounsi, A., Bouremana, M. "Wave dispersion properties in imperfect sigmoid plates using various HSDTs", Steel and Composite Structures, 33(5), pp. 699–716, 2016.
https://doi.org/10.12989/scs.2019.33.5.699

[47] Akavci, S. S. "An efficient shear deformation theory for free vibration of functionally graded thick rectangular plates on elastic foundation", Composite Structures, 108, pp. 667–676, 2014.
https://doi.org/10.1016/j.compstruct.2013.10.019